AGU100 ADVANCING EARTH AND SPACE SCIENCE

Water Resources Research

RESEARCH ARTICLE
10.1029/2017WR021606

Snow Depth Structure, Fractal Behavior, and Interannual Consistency Over Haut Glacier d'Arolla, Switzerland

I. Clemenzi[1], F. Pellicciotti[1,2,3], and P. Burlando[1]

[1]Institute of Environmental Engineering, ETH Zurich, Zurich, Switzerland, [2]Department of Geography, Northumbria University, Newcastle upon Tyne, UK, [3]Swiss Federal Institute for Forest, Snow and Landscape Research, WSL, Switzerland

Key Points:
- Glacier snow depth patterns show fractal characteristics, with two distinct scaling regions separated by a scale break
- Fractal parameters are similar in the two analyzed years, indicating consistent snow depth patterns at the end of the winter season
- Snow depth patterns are markedly different on the glacier tongue and in the upper catchment

Supporting Information:
- Supporting Information S1

Correspondence to:
F. Pellicciotti,
francesca.pellicciotti@wsl.ch

Citation:
Clemenzi, I., Pellicciotti, F., & Burlando, P. (2018). Snow depth structure, fractal behavior, and interannual consistency over Haut Glacier d'Arolla, Switzerland. *Water Resources Research*, *54*, 7929–7945. https://doi.org/10.1029/2017WR021606

Received 28 JUL 2017
Accepted 18 MAY 2018
Accepted article online 7 JUN 2018
Published online 18 OCT 2018

Abstract Snow depth patterns over glaciers are controlled by precipitation, snow redistribution due to wind and avalanches, and the exchange of energy with the atmosphere that determines snow ablation. While many studies have advanced the understanding of ablation processes, less is known about winter snow patterns and their variability over glaciers. We analyze snow depth on Haut Glacier d'Arolla, Switzerland, in the two winter seasons 2006–2007 and 2010–2011 to (1) understand whether snow depth over an alpine glacier at the end of the accumulation season exhibits a behavior similar to the one observed on single slopes and vegetated areas; and (2) investigate the snow pattern consistency over the two accumulation seasons. We perform this analysis on a data set of high-resolution lidar-derived snow depth using variograms and fractal parameters. Our first main result is that snow depth patterns on the glacier exhibit a multiscale behavior, with a scale break around 20 m after which the fractal dimension increases, indicating more autocorrelated structure before the scale break than after. Second, this behavior is consistent over the two years, with fractal parameters and their spatial variability almost constant in the two seasons. We also show that snow depth patterns exhibit a distinct behavior in the glacier tongue and the upper catchment, with longer correlation distances on the tongue in the direction of the main winds, suggesting spatial distinctions that are likely induced by different processes and that should be taken into account when extrapolating snow depth from limited samples.

1. Introduction

Snow depth patterns over complex mountainous terrains are highly heterogeneous (e.g., Clark et al., 2011; Liston et al., 2007; Mott et al., 2010) and controlled by multiple processes acting at different scales: (i) heterogeneous precipitation patterns, determined by winds and the modification of air flows induced by the orography, which are effective at both the local (Dadic et al., 2010a; Lehning et al., 2008) and the mountain range scale; (ii) the redistribution of deposited snow by wind (Schirmer et al., 2011) and/or the canopy interception of snow (Deems et al., 2006; Trujillo et al., 2007, 2009); (iii) the gravitational redistribution by avalanches, which is important in locations of steep relief (Gruber, 2007); and (iv) the energy exchange at the snow-atmosphere interface, determined by the dominant meteorological forcing and its interaction with topographic factors such as exposure and slope, which affects snowpack surface and internal energy budget, thus controlling melt rates and their spatial and temporal variability. Spatial and temporal variability of snow distribution influences snow melt patterns, mass balance distribution and runoff timing (Anderton et al., 2004; Dadic et al., 2008; Egli et al., 2012; Kerr et al., 2013; Luce et al., 1998). While first-order controls on snow patterns have been relatively well established, at least qualitatively, models that can reproduce those spatial and temporal variability still suffer from several limitations. Energy balance snow models require meteorological and surface input data that are rarely available: (i) in situ; (ii) at the spatial resolution compatible with the scale of the dominant processes (Trujillo et al., 2007); and (iii) for long-term simulations. The scale at which snow models work should be selected based on the scales of the processes that models aim at simulating (Trujillo et al., 2007). Knowledge of snow depth patterns and their changes over decadal scales is still limited, as most studies have looked at few years of observations, and a deep understanding of the quantitative controls is still lacking, especially on glaciers. As a result, several hydrological and mass balance models often simulate snow accumulation in a simplified manner (e.g.,Huss et al., 2008; Machguth et al., 2006).

Efforts to characterize snow cover distribution have focused on relationships between snow depth properties and topographic variables such as slope, aspect, and curvatures that can be easily obtained from digital

elevation models (DEMs; Blöschl & Kirnbauer, 1992; Elder et al., 1991, 1998; McGrath et al., 2015). These variables affect the interaction of snow with wind and topography and represent an integrated index of the energy controls that deplete and melt the snowpack. Other studies have sought statistical relationships between snow, topography, and meteorological variables such as wind and radiation (Erickson et al., 2005; Winstral & Marks, 2002; Winstral et al., 2013). However, regression-type relationships are only able to explain a small percentage of the observed variability (Trujillo et al., 2007) and, being based on empirical relationships, are site specific and not valid for environments different from those they have been derived for.

A number of recent investigations have advanced our understanding of snow spatial and temporal variability by employing fractals and scale invariance to analyze the properties of the spatial structure of high spatial resolution snow depth fields (Deems et al., 2006; Schirmer & Lehning, 2011; Trujillo et al., 2007, 2009).

This analysis is usually conducted by way of two approaches: (i) using variograms (Deems et al., 2006; Schirmer & Lehning, 2011) or (ii) looking at the power spectral densities (Trujillo et al., 2007, 2009). Most of the recent investigations on snow spatial scaling and patterns have used the first technique, in which fractal analysis is conducted by looking at the variation in the standard deviation or semivariance of snow depth as a function of sample distance, and fractal dimensions can be calculated from a log-log form of the variogram. Regions where the scaling behavior changes can be identified through scale breaks that indicate distances at which the underlying processes are likely to change. Fractal dimensions and scale break distances also have the advantage that they are quantitative values that can be compared and used to determine whether the fields properties are similar over different periods (or areas). Power spectra of snow depth also provide scale break values (between the two frequency intervals).

There is remarkable agreement among the results of these investigations, which all pointed at a multiscale behavior of snow depth fields with two distinct regions separated by a scale break located at scales of the order of meters to tens of meters (Deems et al., 2006; Schirmer & Lehning, 2011; Trujillo et al., 2007, 2009). A linear law type increase (in the log-log plot) in the semivariance or power spectral density was evident up to sampling distances of the order of tens of meters, after which the relationships tend toward a horizontal line in the log-log plot. This result indicates the existence of two-scaling fractal regimes with a more strongly spatially correlated structure before the scale break. In turn, this suggests the existence of different processes controlling snow accumulation over the two scales, and the scale break distance is typically assumed to be the length at which the underlying processes change (Deems et al., 2006).

The scale break distance is relatively consistent (varying between 6 and 40 m) across study sites, despite differences in physiographic characteristics, geographical regions, and the range of the observed snow depth values. Substantial efforts have been devoted to identify the processes influencing the variation of scale break distance. In vegetated areas, shorter break distances (9–12 m) have been associated with the influence of canopy interception when the effect of wind on snow redistribution was minimal (Trujillo et al., 2007), while longer break distances (15–40 m) were associated to the interaction of wind, vegetation and terrain roughness (Deems et al., 2006). In nonvegetated areas, shorter (6 m) and longer scale break distances (20 m) have been instead explained by the interaction of wind with the terrain roughness in exposed and sheltered mountain slopes, respectively (Schirmer & Lehning, 2011). Among the investigations based on fractal properties, only Arnold and Rees (2003) and Helfricht et al. (2014) have looked at the snow spatial distribution over glacier surfaces. Arnold and Rees (2003) found that the variogram of the snow depth distribution flattened at separation distances between 10 m and 30 m in the summer and 35 m and 45 m in spring, but using a limited sample of manually collected snow depth data. Helfricht et al. (2014) instead did not find a break in the scaling behavior between shorter and longer distances.

Among the numerous recent studies on snow fractal properties, one topic that has been looked at by means of fractal properties is whether snow depth fields exhibit the same spatial structure and fractal properties over time, what has been indicated as *consistency* (Deems et al., 2008) or *persistency* (Schirmer & Lehning, 2011). Fractal dimensions and scale break distances can be compared to determine whether the fields properties are statistically similar over different periods (or different areas), thus hinting at the persistence over time of similar controlling processes. The relevant literature seems to suggest that, in general, snow depth fields seem to exhibit the same spatial structure over time. Deems et al. (2008) found that the estimated fractal parameters in two different years at two sites were consistent and interpreted this result as due to a similar interaction over the two years of the factors that control snow accumulation in those environments: vegetation, wind and terrain. A similar conclusion was reached by Schirmer and Lehning (2011), who found a strong interannual

consistency between the snow depths over an alpine slope at time of peak accumulation in two consecutive winters. The only study at a glacierized site (Helfricht et al., 2014) found contrasting results, as snow cover was found to be persistent over 5 years on the ice-free terrain but not on the glacier surfaces.

Most of the recent studies have taken advantage of the availability of dense, gridded data of snow depth derived from airborne and terrestrial light detection and ranging (lidar) surveys (Helfricht et al., 2014; Mott et al., 2010; Schirmer & Lehning, 2011; Trujillo et al., 2007), in contrast to the less rich data sets of manual measurements (e.g., Arnold & Rees, 2003). This made it possible to cover larger areas with denser intervals as compared with manual probing (Deems et al., 2013) and to achieve a higher accuracy.

In this paper, we analyze snow depth data collected on the Haut Glacier d'Arolla, an Alpine glacier in Switzerland, obtained from high-resolution helicopter-borne lidar surveys in the two seasons 2006–2007 and 2010–2011 (section 2). Our two main aims are to (i) investigate the scaling nature of the data sets and (ii) test whether the fractal characteristics are consistent over the two seasons. We postulate that topography and meteorological forcing control at least in part the obtained patterns, and for this we analyze the concurrent meteorological conditions in the catchment using data from two permanent automatic weather stations (AWSs), focusing in particular on wind speed and direction (section 2).

2. Study Site and Data

2.1. Study Site

Haut Glacier d'Arolla is a small valley glacier located in the southwestern part of the Swiss Alps (Figure 1a). The catchment area is approximately 13 km^2, of which about 6.3 km^2 is glacierized (48% of the watershed area). The elevation range spans between 2,500 and 3,800 m above sea level (asl). Two permanent AWSs, hereafter denoted as T1 and T2 (Figure 1a), provide the meteorological data to characterize the two seasons. T1 is located at 2,600 m asl and about 900 m from the glacier snout, while T2 lies on the Eastern slopes of the glacier, in a flat area sheltered to the north by surrounding peaks (Figure 1a).

2.2. Meteorological Observations

Meteorological data from the two AWSs in the period between the two lidar acquisitions are analyzed to characterize the meteorological conditions in the two accumulation seasons. The two AWSs recorded air temperature, relative humidity, incoming and reflected shortwave radiation, incoming and outgoing longwave radiation, wind speed and direction, and precipitation. T2 is additionally equipped with an ultrasonic depth gauge (UDG), which provided snow depth measurements. All measurements were recorded at a 5-min interval and aggregated to hourly values for this analysis. In particular, for this study we examined precipitation, snow depth, air temperature, wind speed, and wind direction. We corrected precipitation measurements for wind-induced undercatch losses using the approach developed by Nešpor and Sevruk (1999) as reported for an automatic unshielded precipitation gauge by Zweifel and Sevruk (2002). The approach accounts for wind-induced losses with correction factors varying as a function of wind speed, precipitation phase, and intensity.

2.3. Lidar DEMs

Snow accumulation over the catchment was obtained as the difference between two high-resolution DEMs generated from helicopter-borne lidar measurements carried out at the beginning and at the end of the accumulation season in the two years. The lidar measurements were acquired during surveys on 1 November 2006 and 15 October 2010 (beginning of accumulation season) and 1 May 2007 and 6 May 2011 (end of accumulation season). The helicopter-borne lidar technology was based on a portable system integrating a high-resolution digital camera (H1D) and an airborne laser scanner (Riegl LMS-Q240i) with high-accuracy global positioning system and inertial navigation sensors (iMAR FSAS; Skaloud et al., May 2006). Once the raw data were acquired, spurious data and noise were removed to obtain only returns of the ground, snow, and ice surfaces. These were then filtered with a point-thinning technique to deal with the returns from cliff overhanging sections. The planar representation of these landscape features can produce different elevations in correspondence of the same point position and generate spikes and artifacts in the terrain model. For this purpose a *z* tolerance algorithm, which kept the highest point in a defined cell size, was used (J. Vallet, personal communication, 2013). The point-thinning procedure reduced the size of the data, but maintained constant the point density (around 3–4 pts/m^2). Each thinned data set was then used to generate a triangulated

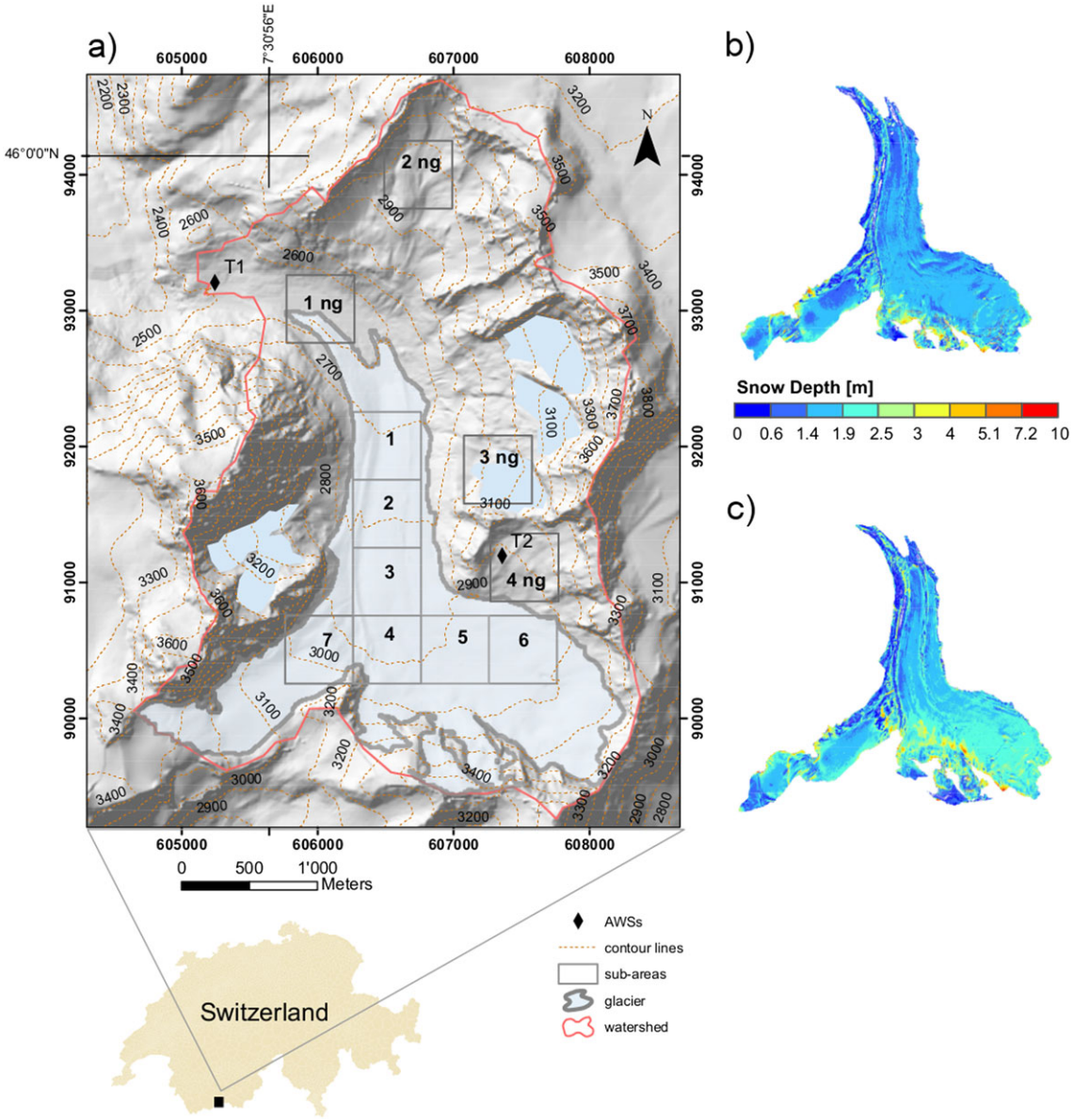

Figure 1. Map of Haut Glacier d'Arolla (a) showing the glacier, the catchment, the subareas used for the analysis of the spatial differences and the position of the Automatic Weather Stations (AWSs) T1 and T2 (measured grid in Swiss Coordinate System CH1903; crosshair in WGS84). Snow depth maps in the years 2007 (b) and in 2011 (c).

irregular network (TIN) from which the final DEM at 1 m grid resolution was produced (J. Vallet, personal communication, 2013). The horizontal and vertical accuracy of each DEM is 0.10–0.15 m and 0.08–0.10 m for the acquisitions in 2006–2007 and 2010–2011, respectively (J. Vallet, personal communication, 2013).

2.4. Snow Depth Data

Snow depth distributions obtained as difference between each pair of DEMs exhibited some negative values and some high positive values. The high positive values were found by visual inspection to be limited to the DEM borders, while negative values were present on the catchment steep slopes and where the terrain roughness was high, for example, in correspondence to the western lateral and medial moraines of the glacier. Positive values are artifacts due to the different elevation values assumed by the cliff overhanging sections in each of the two initial DEMs. Negative values imply that the surface at the end of the accumulation season is lower than the one at the beginning. On the steep slopes this can be the result of the combined effect of the data accuracy and the error introduced by the interpolation to produce snow-covered and snow-free surfaces. This latter type of error is also related to the terrain surface complexity (Deems et al., 2013).

Negative values represented only a small percentage (about 2%) of the total amount of points and over the glacier this percentage was even smaller (about 0.01%). The numbers of points with snow depth higher than 10 m, which is the maximum amount estimated at the foot of the slopes and in correspondence of crevasses, was about 0.3% of the total amount of grid points. As both types of values were a small percentage of the total amount of grid points, they were not considered in the analysis of snow depth spatial properties on the glacier and in seven subareas of equal area covering the main glacier (Figures 1a–1c).

3. Methods

The concept of fractal geometry was formalized by Mandelbrot (1977, 1982) to describe self-similarities of natural geometric patterns across scales. Fractal objects can be characterized by scale invariance, that is, parts of the object preserve the geometrical or statistical characteristics of the whole under scale transformations (Mandelbrot, 1982). The scaling relationship of the fractal object with its geometrical or distributional characteristics under scale transformations is quantitatively described by the fractal dimension. This describes the topology of an object in the fractal space quantifying the magnitude of the complexity or irregularity of the fractal object (Mandelbrot, 1977, 1982). In contrast to the spatial dimension in the Euclidean geometry, the fractal dimension can assume any noninteger value, for example, values between 1 and 2 for a curve and between 2 and 3 for a surface. A surface fractal dimension can be any noninteger value between 2 and 3, with an infinitely rugged (complex) surface having a fractal dimension of 3 and a perfectly smooth surface a fractal dimension of 2. Low-surface fractal dimension values have been thus interpreted as characterizing smooth and persistent structures, and high fractal dimension values as representative of rugged and nonpersistent structures. In contrast to mathematical objects, natural patterns showed a fractal behavior, that is, self-similarity or, more in general, self-affinity, over limited regions, ranges of scale and over more than one scaling region (e.g., Klinkenberg & Goodchild, 1992; Mark & Aronson, 1984; Sun et al., 2006). Similarly to the patterns of other variables describing natural phenomena or processes, snow depth fields also have been shown to have more than one scaling region. In this case, the fractal dimension can still be used to describe the variability over different scaling windows and the length of change in spatial variability (scale break length), often associated with the influence of physical processes acting at different scales (Deems et al., 2006; Schirmer & Lehning, 2011; Trujillo et al., 2007). The fractal dimension and the length of change in the spatial variability have been mostly derived from the shape of the variogram function (Arnold & Rees, 2003; Deems et al., 2006; Schirmer & Lehning, 2011; Shook & Gray, 1996). In this study we follow the same approach to investigate the fractal behavior of the snow depth distribution over the glacier and we consider the snow depth distribution having a certain degree of spatial organization until the maximum sample distance.

The empirical variogram expresses, on average, the relationship between the variance of the observations, $\gamma(h)$, and their separation distance, h. It is formally defined by the following equation:

$$\hat{\gamma}(h_k) = \frac{1}{2N(h_k)} \sum_{(i,j)\in h_k} \left(z_i - z_j\right)^2 \tag{1}$$

where z_i and z_j are the snow depth observation pairs and $N(h_k)$ is the total number of such pairs in the lag distance class h_k (Webster & Oliver, 2007).

In case of scale invariance, or more in general self-affinity, the variogram of a variable is described by a power law

$$\gamma(h) = ah^b \tag{2}$$

The exponent b is related to the fractal dimension of the surface, D, through the equation:

$$D = 3 - b/2 \tag{3}$$

and it can be estimated from the slope of the least-square fitted linear function that fits the dependence of the semivariance on the lag distance in the log-log scale (Gao & Xia, 1996).

The variogram can be used to explore the semivariance of the observations as a function of distance classes only (the so-called omnidirectional variogram) or by looking at these classes in a given direction (the so-called

directional variogram). In this analysis, both omnidirectional and directional variograms are calculated for the snow depth over the entire glacier and in each of the glacier subareas. The directional variograms are calculated to detect possible anisotropy in the snow depth spatial distribution and thus differences of the fractal dimension with direction.

The snow depth fields used to compute the omnidirectional and directional variograms in the glacier subareas are used at the best spatial resolution (1×1 m), while the snow depth used to calculate the omnidirectional variograms over the entire glacier are resampled to 5×5 m resolution, which represents the best compromise between representativeness and computational demand. The maximum distance considered in the variogram calculation was set equal to half of the maximum point pairs distance for the computation of the variogram over the whole glacier and to the maximum distance of 500 m for the computation of the variogram over the subareas. Following Deems et al. (2006) and Schirmer and Lehning (2011), we divided the maximum distance in 50 log-width intervals. The higher amount of bins at short distance obtained in this way in comparison with the linear width allows to better identify the correlation structure at shorter scales and to improve the variogram fitting.

Directional variograms were computed for 16 classes each of 22.5°. Theoretical variograms were then fitted to the empirical variograms with a piecewise linear regression function which minimizes the sum of the square residuals. This guarantees the continuity of the modeled function when changes in the semivariance slope occur and different scaling regions can be identified. The distance at which the slope of the fitted variogram changes corresponds to the scale break distance, L, while the scaling behavior before and after the scale break can be characterized through the fractal dimensions, indicated as D_s and D_l, respectively, for the short and the long regions. These metrics are used to describe the fractal behavior of the snow depth fields and to compare their similarities.

We also analyzed the fractal structure and fractal parameters for four subareas, of 500 × 500 m, located outside of the glacier surface, to assess differences in spatial structure compared to the glacier areas and potential influences of glacier characteristics on the spatial scaling patterns of snow depth. We defined four areas of snow-covered terrain on the slopes and in the proglacial valley (Figure 1), which we selected to have the most similar range of slopes to the glacier subareas, to limit the effect of steep slopes on the accuracy of snow depth data and given that slope can significantly affect snow redistribution by gravity. For the four off-glacier subareas, we calculated the main statistics, the omnidirectional variogram and the fractal parameters as for the glacier subareas, for the snow depth distribution in 2011.

4. Results

4.1. Meteorological Forcing

Daily cumulative precipitation corrected for undercatch losses at the automatic weather station T2 is shown in Figure 2a. It is evident that precipitation amounts (between November and April) are higher in 2010–2011 than in 2006–2007. The same was found also for the uncorrected measurements (not shown). Snowfalls during the first months of the accumulation period are more frequent in 2010 than in 2006 (Figures 2a and 2c) and a deeper snowpack is present in 2010–2011 (Figure 2b). In both seasons, air temperature remains below zero for most of the period of record (Figure 2d), thus favoring redistribution of deposited snow by wind (Trujillo et al., 2007). The daily average temperature over the period of record is −8.2 °C in 2010–2011 and −6.1 °C in 2006–2007. Sustained negative temperatures (Figure 2d) suggest that little melt had occurred before the lidar surveys in both years. To corroborate this, we calculated melt and snow water equivalent at the location of T2 (Figure 1) using the physically based snowpack model Crocus (Brun et al., 1989, 1992; Vionnet et al., 2012) for the two accumulation periods. The estimated cumulative melt in the period between 1 March, when an increase of air temperature is observed, and the second survey at the peak of accumulation, is 9 mm in 2007 and 7 mm in 2011. These are very small values, which suggest that, at least in the upper areas of the glacier, snow depth patterns have not been affected by melt.

Following Deems et al. (2008), we computed wind direction frequencies at both stations for two subsets of data, namely, those corresponding to precipitation events only, that is, when a daily precipitation amount different from 0 is measured (Figure 3) and those corresponding to wind speed observations larger than 5 m/s only (Figure 4).

Wind directions are remarkably consistent in the two winters. During precipitation events, wind at T1 mostly comes from the east and east southeast in both seasons (Figure 3a), indicating that the air flow follows the

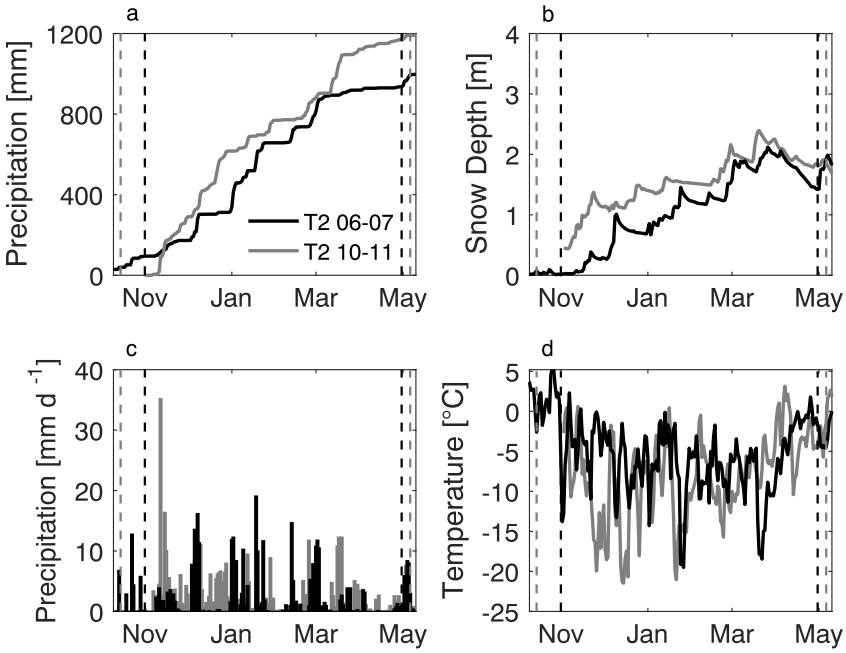

Figure 2. Daily meteorological data of (a) cumulative precipitation corrected for undercatch losses induced by wind, (b) snow depth, (c) measured precipitation, and (d) average air temperature from the automatic weather station T2. Dashed lines indicate the dates of the lidar flights.

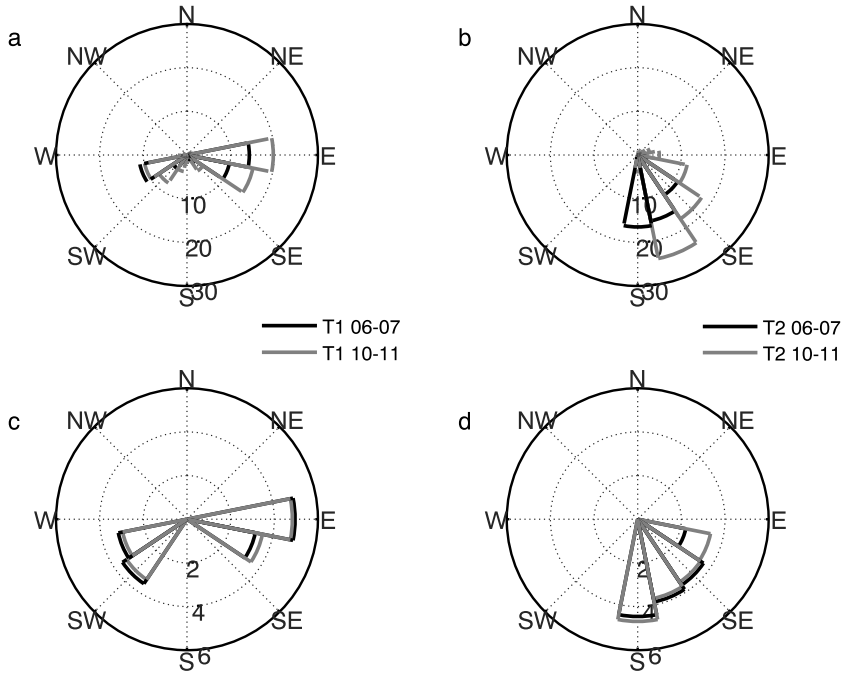

Figure 3. Wind direction frequencies at the meteorological stations T1 and T2 for precipitation events only (a, b) and the correspondent mean wind speed (c, d) in the period November–April in the years 2006–2007 and 2010–2011.

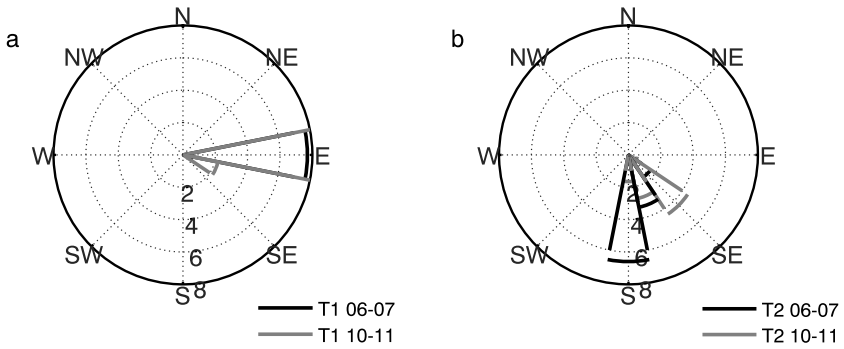

Figure 4. Wind direction frequencies at the meteorological stations T1 and T2 (a, b) for wind speed higher than 5 m/s, in the period November–April in the years 2006–2007 and 2010–2011.

main glacier flow line direction, likely because of the strong topographic channeling effect. The highest average wind speed is observed when the prevailing wind is from the east in both seasons (Figure 3c). At T2, wind comes prevalently from the southern quadrant in both seasons (Figure 3b). At T2, mean wind speed is slightly higher when wind comes from the south than from the other directions in the season 2006–2007, while in 2010–2011 mean wind speeds are rather homogenous across directions (Figure 3d). For wind speed larger than 5 m/s (Figure 4), at T1 the wind is mainly from the east in both years (Figure 4a), while at T2 the prevailing wind direction slightly differs from one season to the other, with southeasterly winds in 2006–2007 and south southeasterly in 2010–2011 (Figure 4b). The prevailing wind directions corresponding to wind speed larger than 5 m/s are consistent with those identified for precipitation events only, suggesting that high wind speeds are observed at both stations in correspondence or immediately after precipitation events.

4.2. Snow Accumulation From Lidar

The distribution of snow depth is shown in Figure 5 for both the entire glacier and the seven subareas of 500 × 500 m. The median of the distributions is higher in 2011 than in 2007, and the dispersion around the median, represented by the box boundaries, is slightly higher in 2011 than in 2007. A trend is evident in the snow depth distribution over the glacier in the two seasons: the median snow depth increases from the tongue (subareas 1–3) to the subareas of the southeastern part of the upper catchment (4–6). The highest values of the median and mean correspond to subareas 4 to 6 both in 2007 and in 2011 (Table 1). This trend is more marked in 2011 than in 2007. The smallest spreads of the distributions are found in correspondence of subareas 5 and 6 in both years.

The lowest and the highest snow depth variability correspond to subareas 5–6 and 1–7, respectively (Table 1). When comparing the subareas' snow depth distributions to the one computed for the entire glacier, the median snow depth in subareas 1–3 and 7 is below the value for the entire glacier in both seasons, while the median snow depth in the upper catchment is higher or of the same magnitude.

Table 1
Mean, Standard Deviation (Std), and Coefficient of Variation (CV) of the Snow Depth Distribution Over the Entire Glacier and in the Glacier Subareas in the Two Years

	2007			2011		
	Mean [m]	Std [m]	CV	Mean [m]	Std [m]	CV
Glacier	1.51	0.40	0.34	1.8	0.45	0.33
Subarea 1	1.20	0.51	0.43	1.35	0.66	0.49
Subarea 2	1.30	0.29	0.26	1.50	0.46	0.31
Subarea 3	1.38	0.27	0.21	1.58	0.34	0.22
Subarea 4	1.56	0.33	0.30	2.0	0.57	0.29
Subarea 5	1.44	0.24	0.13	1.87	0.22	0.11
Subarea 6	1.40	0.25	0.20	1.84	0.26	0.14
Subarea 7	1.35	0.81	0.50	1.65	0.89	0.54

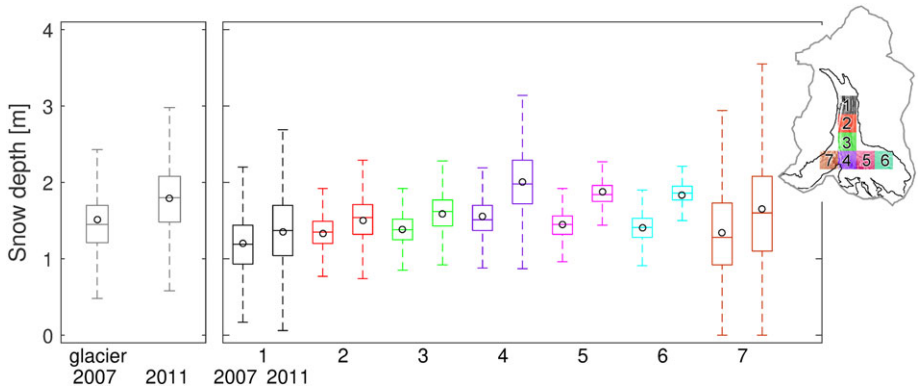

Figure 5. Snow depth distributions over the entire glacier and in the glacier subareas (1–7) for the two seasons 2006–2007 and 2010–2011. The central mark of each box is the median, the edges of the box are the 25th and 75th percentiles, the whiskers extend to the points obtained according to $q_{0.75}$ + 1.5($q_{0.75}$ - $q_{0.25}$) and $q_{0.25}$ - 1.5($q_{0.75}$ - $q_{0.25}$), where $q_{0.25}$ and $q_{0.75}$ are the 25th and 75th percentiles, respectively. Values beyond the whiskers lengths are not shown. Circles show the mean of the distributions.

The spatial correlation of the snow depth distribution is shown in Figure 6 for an area of 200 × 200 m centered in each of the seven glacier subareas and calculated up to *x* lag and *y* lag of ±100 m. There are clear differences in correlation structure between the areas on the glacier tongue and in the upper section. On the glacier tongue (subareas 1 and 2), the two-dimensional correlograms show an anisotropic decay, reaching the value of 0.4 for a lag of the order of 50 m in the north-south direction (Figure 6). This finding indicates that small-scale variability prevails in the direction east-west, while longer scale variability prevails in the north-south direction in these subareas. In the upper catchment instead, the correlation function of the snow depth shows little anisotropy with ring-shaped contour lines up to a correlation function value of 0.2 for lags of the order of 15 m (subarea 5; Figure 6). The spatial differences in the snow depth correlation structure between the tongue and the upper catchment subareas are temporally consistent in the 2007 and in 2011.

4.3. Snow Depth Variograms

4.3.1. Omnidirectional Variogram of the Glacier Snow Depth

Omnidirectional variograms of the glacier snow depth in the log-log scale are shown in Figure 7. In both seasons snow depth shows a scaling behavior with two characteristic domains where the semivariance between

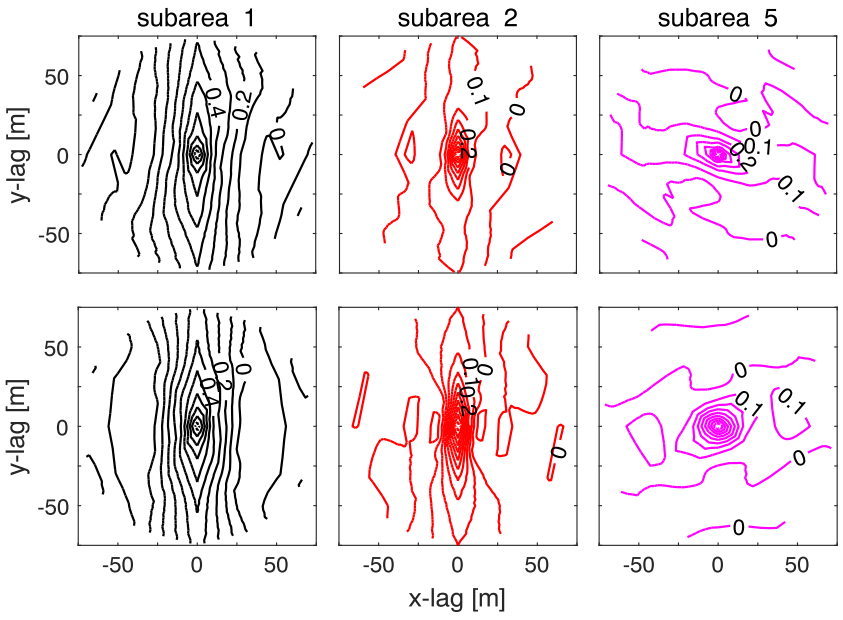

Figure 6. Two-dimensional correlogram of the snow depth distribution in the subareas 1, 2, and 5 in the years 2007 (top row) and 2011 (bottom row).

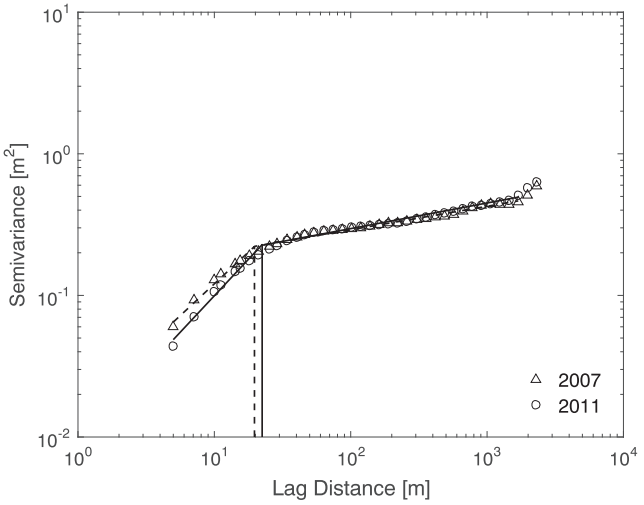

Figure 7. Omnidirectional variogram of the glacier snow depth for the two years. The dashed (2007) and solid (2011) vertical lines indicate the scale break distance (*L*) for the two years.

neighboring snow depths, rapidly increases up to a distance of about 20 m and less rapidly after, as indicated by the slope of the fitted linear variogram in the log-log space. For both seasons, fractal dimensions are about 2.5 and 2.9 before and after the scale break, respectively (Table 2). A lower fractal dimension at short distances indicates that the snow depth spatial structure is more autocorrelated before the scale break than after.

4.3.2. Omnidirectional Variogram of the Subareas Snow Depth

Omnidirectional variograms of the snow depth in the log-log scale show a scaling behavior with two characteristic domains for all sub areas (Figure 8). This behavior is consistent between the two years across the majority of the subareas, with the only exception of subarea 7. Except for the snow depth distribution in this subarea, distributions in all the other subregions are characterized by similar D_s and D_l (Table 2), with the short range fractal dimensions varying between 2.49–2.66 and 2.57–2.76 in 2007 and in 2011, respectively (Table 2). Even if D_s is slightly higher in 2011 than in 2007, D_s varies in a similar manner from the subareas 1 to 5 in both seasons (Figure 9a). In particular, a clear difference, consistent in the two years, is evident between the glacier tongue (subarea 1) and the upper catchment (subareas 4 and 5), with D_s values increasing from the glacier tongue (subarea 1) to the upper catchment (subareas 4 and 5). Variability is less marked for the long-scale fractal dimension, D_l, which ranges between 2.88 and 2.97 (Table 2) and is rather constant across subareas. The length of the scale break, *L*, varies for all the subareas between 10 and 35 m (Figure 9b). The scale break distance is smaller on the glacier tongue (sub-area 1-3) than in the upper catchment (sub-area 4, 5 and 7) and, for the same sub-area, is lower in 2007 than in 2011 (Figure 9 and Table 2).

4.3.3. Directional Variogram of the Subareas Snow Depth

Exploiting the dense and uniformly spaced grid of data points provided by the lidar data sets, we also calculated directional variograms for different angle classes to explore the fractal dimension dependence on direction and identify the presence of possible anisotropies. Figure 10 shows the directional variograms in the log-log scale of the snow depth computed for two selected directions, north-south (0°) and east-west (90°), for the year 2011. In these two directions, the scaling behavior appears significantly different between the areas of the glacier tongue (subareas 1a and 2) and those of the upper catchment (subareas 5 and 6), with the subareas 3 and 4 showing an intermediate behavior. On the glacier tongue the scale break occurs at shorter distances and the semivariance is higher in the east-west direction than in the north-south. The difference between the fractal behavior in these two directions becomes less evident for the subareas 3 and 4 and not noticeable for the subareas of the upper catchment. On the glacier tongue, the short-range fractal dimension

Table 2
Fractal Dimension Values of the Snow Depth at the Short and the Long Range for the Glacier Subareas for the Two Years

	2007			2011		
	Ds	Dl	*L* (m)	Ds	Dl	*L* (m)
Glacier	2.49	2.94	20	2.55	2.94	22
Subarea 1	2.49	2.94	15	2.57	2.92	22
Subarea 2	2.49	2.96	12	2.53	2.97	17
Subarea 3	2.55	2.95	10	2.61	2.91	18
Subarea 4	2.60	2.94	13	2.63	2.91	25
Subarea 5	2.66	2.91	17	2.67	2.88	30
Subarea 6	2.55	2.97	14	2.68	2.97	22
Subarea 7	2.60	2.93	22	2.76	2.97	35

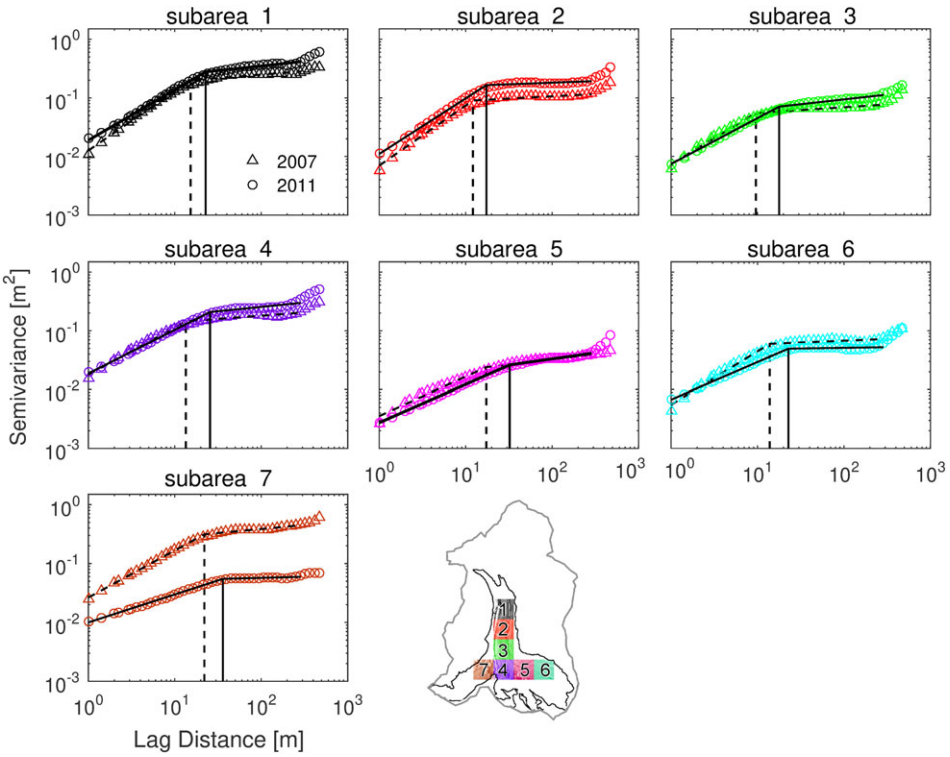

Figure 8. Omnidirectional variogram of the snow depth in the seven glacier subareas for the two years. The dashed (2007) and solid (2011) vertical lines indicate the scale break distance (L) for the two years.

is larger in the direction north-south compared to the direction east-west. The short-range fractal dimension in the direction north-south is also higher than any other direction (Figure 10).

5. Discussion

5.1. Multiscaling Behavior

Analysis of the omnidirectional variograms has shown that the snow depth has a multiscaling structure both when the entire glacier and the glacier subareas are considered. This result is in agreement with most studies on snow covered but not glacierized sites, which found multiscaling behavior of snow depth across locations of different size, elevation, latitude, and land cover (Deems et al., 2006; Schirmer & Lehning, 2011; Trujillo et al., 2007). The glacier and glacier tongue subareas have D_s similar to those found in the previous studies, while in the upper catchment D_s is higher than those found in the previous studies. D_s in the upper catchment above 2.5 indicates a less correlated structure, with short-range variations of small amplitude given the lower snow depth semivariance (subareas 4 to 6) than that of the glacier tongue (subareas 1 and 2). The upper catchment is thus characterized by a less spatially correlated snow depth structure than the glacier tongue. Conversely, the glacier tongue seems to exhibit a more spatially correlated structure ($D_s \approx 2.5$). Analysis of the snow depth

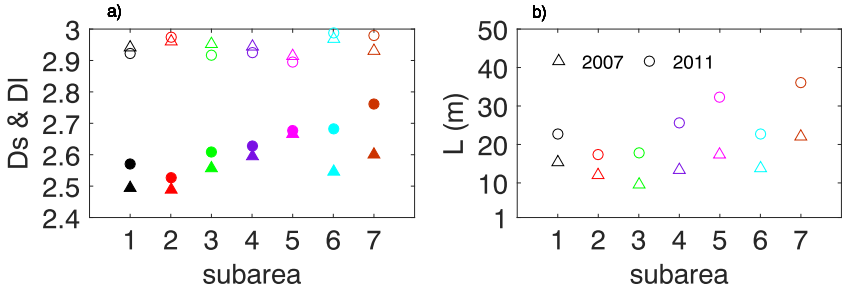

Figure 9. Short (D_s, solid symbol) and long (D_l, open symbol) range fractal dimension (a) and scale break distance (L) (b) for the glacier subareas for the years 2007 and 2011.

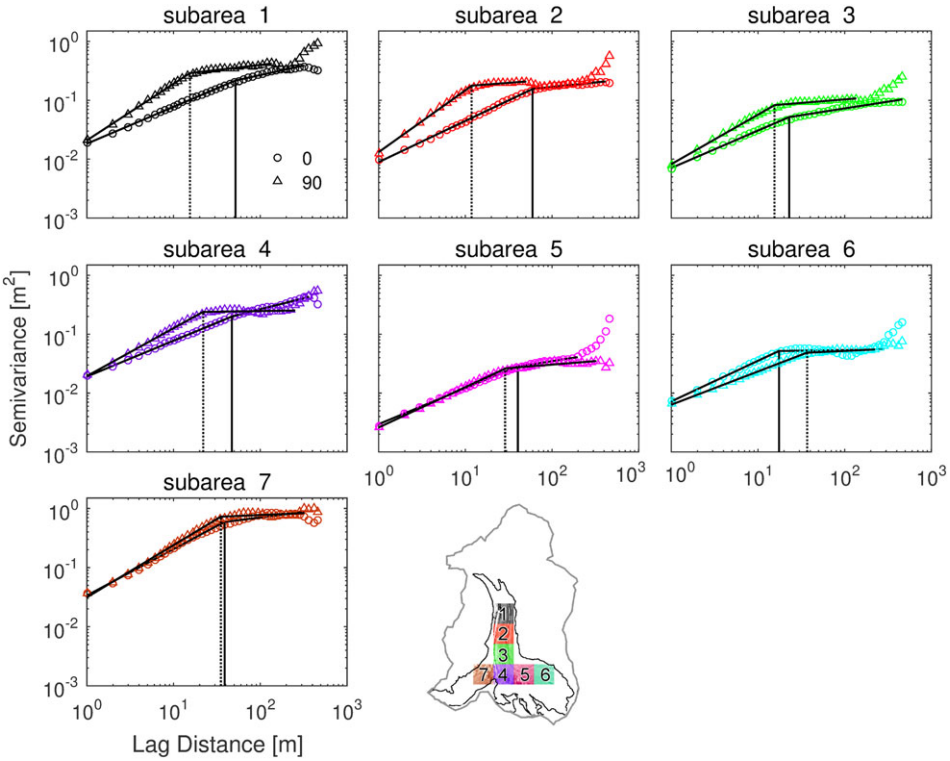

Figure 10. Directional variogram of the snow depth for the glacier subareas in the two directions [north-south (0°) and east-west (90°)] for the year 2011. The solid (0°) and dotted (90°) vertical lines indicate the scale break distance (*L*) for the two directions.

distribution for the four off-glacier subareas in 2011 (Table 2 of the supporting information) shows that the fractal dimension at short and long range on the glacier tongue are similar to those found off glacier.

We also identified a scale break distance below which neighboring observations are autocorrelated and, conversely, weakly correlated or uncorrelated beyond it. We found scale break distances of about 20 m on the glacier in both years when analyzing the entire glacier. Similar scale break distances are found for the tongue subareas (17–22 m), while *L* is larger in the upper catchment (22–35 m) in the year 2011. In 2007 instead, scale break distances were below or about 20 m for most of the glacier subareas, with only small differences between the glacier tongue and upper catchment (Figure 9). Smaller scale break distances in the year 2007 compared to the year 2011 are the results of the increase of the semivariance for lag distances just below the scale break in the year 2007 compared to the year 2011. The range of scale brake distances found on the glacier and in the tongue subareas is similar to those outside the glacier (16–23 m) in 2001. These values are in agreement with those in Helfricht et al. (2014) for ice-free terrain 18–20 m and obtained by Schirmer and Lehning (2011) for a cross-loaded slope (20 m) in mountain terrain. The scale break distances found in the upper catchment are instead similar to those found by Deems et al. (2006, 2008) in a vegetated site with steep terrain above the tree line (26–40 m). Within the range found by previous studies, shorter break distances have been mainly regarded as the result of the interaction between surface features (such as vegetation characteristics or surface roughness), precipitation, and wind pattern (Schirmer & Lehning, 2011; Trujillo et al., 2007), while longer break distances have been suggested to result from the interaction of larger topographic features (relief, terrain concavity, and convexity) with wind pattern (Deems et al., 2006; Trujillo et al., 2007).

While our results are coherent with those reported for snow-covered areas, it is difficult to compare them with those of the other two studies on snow patterns on glaciers. On one hand, the study by Helfricht et al. (2014) on a glacierized catchment in the Austrian Alps did not identify a scale break. The authors investigated the snow depth spatial distribution of the two glaciers Hintereisferner and Kesselwandferner (and of few other small glaciers) in the Ötztal and found no break in the scaling behavior between shorter and longer distances. The snow depth behavior was interpreted as scale-invariant only over 100 m. On the other hand, our findings

are in agreement with the results by Arnold and Rees (2003), who found scaling behavior up to a distance of ≈ 50 m over the midre Lovénbreen (Svalbard, Norway) using snow depth data manually sampled along transects. Their scale break distances for peak accumulation are slightly larger than those we found, and this might be due to different characteristics of the glacier and processes generating the winter snow pack or differences in the sampling approach. These are the two only studies of snow depth fractal properties over glaciers in addition to the one presented here. It is thus apparent that there is a need for further work on the scaling properties of snow over glaciers, to establish whether our results are exceptional for Haut Glacier d'Arolla or represent general features of the glacier snow depth, and to understand under which topographic and climatic conditions fractal scaling patterns can be observed also over glacier surfaces.

5.2. Temporal Persistence

Also in agreement with the results of previous studies that have investigated the temporal stability of snow depth patterns (Deems et al., 2008; Helfricht et al., 2014; Schirmer et al., 2011), fractal dimensions and scale break distances are similar in the two seasons, indicating persistence in the snow depth spatial structure over the two periods. The fractal dimension at the short range is slightly higher in 2011 than in 2007, particularly in the subareas 1, 6, and 7. This is likely related to the lower semivariances in correspondence of the first lag-distances (1 – 3 m), although it is clear that the increase of the semivariance is similar in both seasons.

Such consistent behavior seems to imply that processes generating the observed snow cover spatial organization in the two seasons are similar or interact in a similar way. The recurrence of snow cover patterns across years has been indicated to occur where the main responsible controls change slowly in time, such as for topography and vegetation, or where these *fixed* controls interact with *dynamic* ones, such as meteorological conditions, which show the same characteristics each year (Sturm & Wagner, 2010). Some studies have, in particular, attributed the interannual stability of snow patterns to the recurrence of the prevailing direction of snow storm and drifts (Schirmer et al., 2011; Winstral & Marks, 2014).

The interaction between topography and consistent wind patterns is likely also the explanatory mechanism for the results of this study, as consistent wind patterns have been observed in both seasons during precipitation events (Figures 3a and 3b). Fractal parameters are remarkably similar especially on the glacier tongue where winds have a more defined flow direction (Figure 9) and less so in the upper catchment where wind is less consistent in direction. This area is more opened and less topographically constrained, and thus subject to varying winds of different origins.

5.3. Spatial Variability

While snow depth in the glacier subareas also shows a multiscaling behavior, there is a remarkable difference between the lower and upper sections of the glacier. The short-range fractal dimension on the tongue subareas is higher in the direction north-south compared to the other directions, while no such distinction is evident in the upper section of the glacier. Hence, on the tongue snow depth exhibits in the north-south direction a less correlated structure extending to larger distances. This finding, together with that of a lower value of the short-range fractal dimension in the direction east-west, indicates that on the tongue the short-range variability prevails in the direction east-west, while longer scale variability prevails in the north-south direction. This is evident also in the analysis of the correlation function of the snow depth, which on the tongue subareas decays more slowly in the direction north-south compared to the other directions, while no such anisotropy is evident in the upper section of the glacier (Figure 6).

These results, showing a significant difference between the lower and upper sections of the glacier, support the hypothesis that the interaction between topography and consistent wind patterns is among the explanatory mechanisms of the observed differences. The observed snow depth variability is a result of processes acting at two different scales: the small scale of snow accumulation interacting with small-scale features of the glacier surface and the larger scale of accumulation processes controlled by the larger-scale topography that constrain the general air flow on the glacier. During precipitation events, the prevailing wind directions observed at the permanent automatic weather stations in the period between the two lidar surveys indicate in both seasons the existence of a main flow from the upper catchment down to the proglacial valley along the main flowline (Figures 3a and 3b). Due to the topographic constraint exerted by the surrounding mountains this corresponds to an air flow in the direction north-south over the tongue, while the wider shape of the upper catchment favor winds from varying directions. Recent modeling results (Clemenzi, 2016) with the mass-consistent model WINDS (Burlando et al., 2007) have shown wind to be north-south oriented on the glacier tongue and less so in the upper catchment (Clemenzi, 2016).

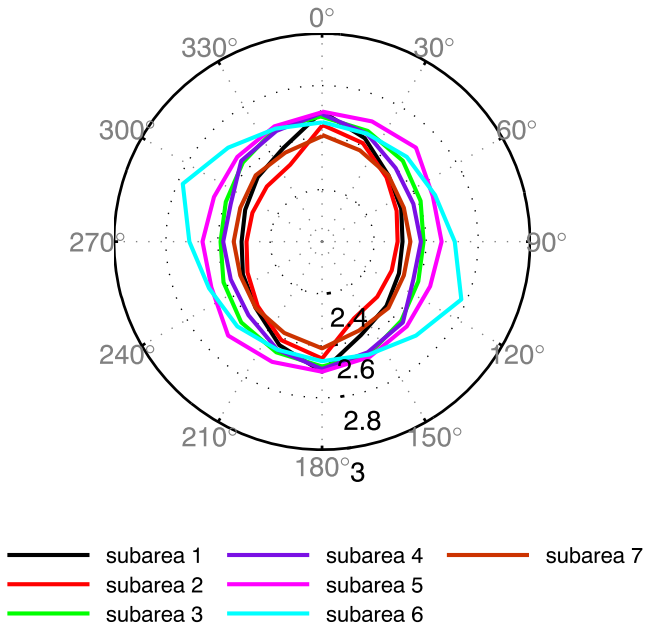

Figure 11. Short-range fractal dimension of the snow depth by angular distances for the glacier subareas for the year 2011.

Several previous studies found wind to have a strong influence on snow depth patterns and their observed anisotropy and directionality. Our finding of largest short-range fractal dimension in the direction parallel to the prevailing wind direction differs from two previous studies, which found largest values of D_s corresponding to the direction perpendicular to the prevailing wind direction (Deems et al., 2006; Schirmer & Lehning, 2011). The difference with the study by Deems et al. (2006) can be attributed to the presence of vegetation in that study case, which acted as an obstacle for the wind and was thus able to create more spatially persistent patterns in the short range region. In contrast to the study by Schirmer and Lehning (2011), which found this result for the cross-loaded catchment slope (i.e., the slope loaded by the prevailing storms), the glacier is an area where horizontal and vertical wind velocity variations occur less abruptly compared to the catchment slopes regardless of the dominant storm direction (Clemenzi, 2016; Dadic et al., 2010b).

This condition can favor the generation of a snow depth spatial structure extending to larger scale that reflects snow accumulation processes at larger scale, for example, the precipitation deposition controlled by the wind patterns and large-scale topography, as it occurs on the tongue along the flow direction and in the upper catchment. Topographic relief has been suggested by Deems et al. (2006) to be among the factors explaining longer scale break. In addition, little or no redistribution by wind has been associated to little or no directionality in the fractal properties of snow (Trujillo et al., 2007), a finding that agrees with our results from the upper sections of the glacier (Figures 10 and 11).

Larger scale has been instead found to explain the majority of the snow depth variability in wind-dominated environments by Trujillo et al. (2007). They found higher contributions of the larger-scale frequency to the variance of the snow depth profile along the predominant wind directions and the lowest along the perpendicular direction. This behavior was associated to the vertical interaction of wind patterns with obstacles such as ridges and depressions (and clusters of vegetation when present) along the predominant wind direction, while to the horizontal interactions of wind patterns with obstacles such as rocks and trees (when they occur). The scales of these processes depend on the separation distances between obstacles, on the wind velocities and surface conditions (Trujillo et al., 2007). The results of our study are in agreement with the finding that snow depth variability at longer distances dominates in our case along the main glacier flowline, while the variability at shorter distance dominates in the perpendicular direction on the glacier tongue. In contrast, no significant differences are visible in the semivariance of the snow depth beyond the scale break between the two directions. This different finding compared to that of Trujillo et al. (2007) is likely due to the fact that on the tongue, where anisotropy in the snow depth correlation and fractal properties was found, pronounced glacier surface irregularity are mainly oriented in the direction parallel to the wind flow.

Analysis of the directional variograms of the DEM in snow-free conditions shows the topography structure of the glacier tongue subareas as characterized by two scaling domains in the direction east-west, which do not appear in the direction north-south (Figure 12). The scale break in the direction east-west is compatible with the presence of these glacier surface features such as the lateral and medial moraines. However, correlation breaks in the glacier surface elevations are at a longer distance and the fractal dimensions are lower compared to those of the snow depth distributions. In contrast, the topography structure of the glacier tongue subareas does not show any scale break in the direction north-south. This suggests that the fast decay of the snow depth correlation in that direction is influenced by other factors. Similarly to moraines, meltwater channels are glacier surface features that, if not covered at the time of the first lidar survey, can contribute to generate snow depth small-scale variability (Helfricht et al., 2014). The glacier tongue sub-areas are also those more influenced by snow avalanches as laterally confined by the catchment mountain slopes. These features, being longitudinally oriented, can generate shorter scale break in the direction east-west.

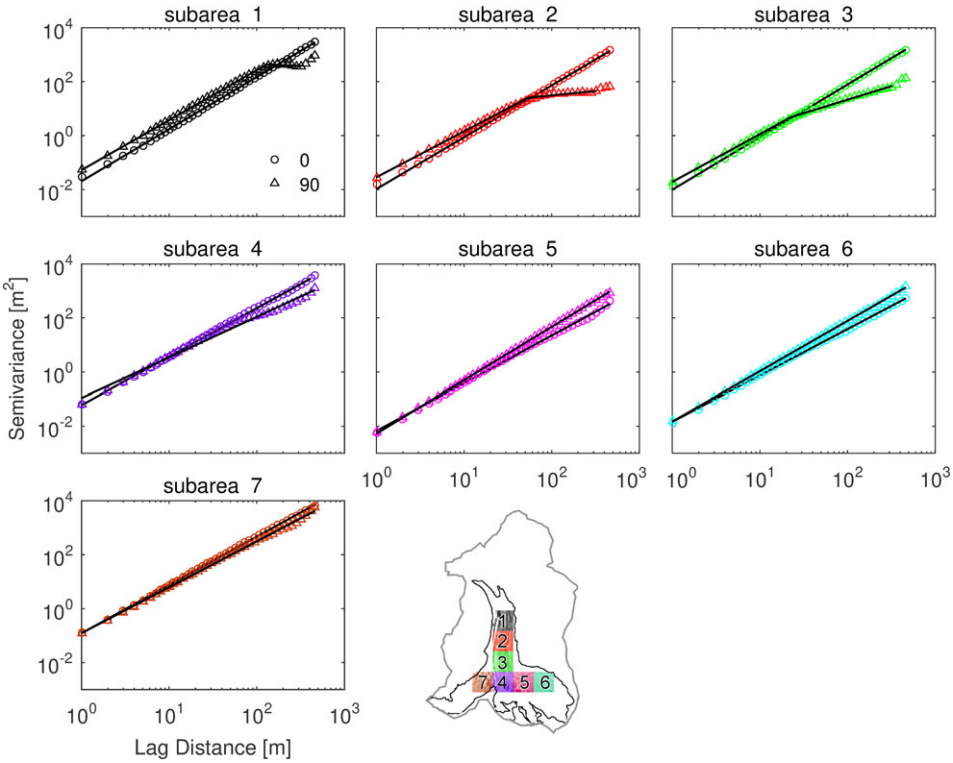

Figure 12. Directional variogram of the glacier topography (in October 2010) for the subareas in the two directions north-south (0°) and east-west (90°).

5.4. Relevance and Implications

While wind seems to be a dominant mechanism to explain snow depth patterns and anisotropy, the deterministic causes generating those patterns, including the actual wind distribution on a glacier and the characteristics of wind-controlled redistribution and energy exchange processes, need more investigation. In absence of high-resolution intraseasonal measurements, which could shed light on the evolution of the seasonal snowpack, the actual mechanisms and causes of our results can only be investigated using models including all relevant physical processes (e.g., Lehning et al., 2008; Liston et al., 2007). Our results provide one of the first assessments of the characteristic scales of snow depth over glaciers. The scale break, separating two distinct scaling and correlation regimes, is an important indication of the scales at which models should work (Trujillo et al., 2007). When snow is analyzed at scales smaller than the scale break, the variability at small scales controlled by small-sale interaction becomes dominant (Trujillo et al., 2007). The scale at which snow models work should be selected based on the scale break and the type of processes that models aim at simulating. Since scales are expected to change with the characteristics of glacier environments, it seems important to extend the analysis carried out here to other glaciers with distinct elevation ranges, flow regimes, surface properties and climate, to compile, as it has been done for snow, a robust range of characteristic scales.

Our results on temporal persistence are encouraging, since they suggest that wind is a key control of anisotropy and scaling properties and that once the actual controls are identified through rigorous physically based modeling, they seem to be stable in time and could be parameterized or modeled with simpler approaches than those including the full range of snow transport processes, which due to the complexity of the model equations and computational burden cannot be used for long-term model simulations.

6. Conclusions

In this paper, we have analyzed two gridded data sets of glacier snow depth at the peak accumulation, derived from helicopter-borne lidar surveys, with the aim of investigating if they exhibit fractal distributions and if their fractal properties are interannually consistent. There is only another recent study (Helfricht et al., 2014) that analyzed snow depth patterns and their scaling properties on a glacier using high-resolution lidar data sets. We extended the range of their investigation by looking closely at the snow spatial structure over different

regions of the glacier (seven subareas selected to cover the main glacier), and over the accumulation and the ablation area, in particular, and by investigating the directionality and anisotropy of the scaling and fractal properties of the snowpack.

Our main conclusions are as follows:

1. In agreement with previous studies over mountain slopes, we found that also on a glacier snow depth shows fractal characteristics, with two distinct scaling regions separated by a scale break. This indicates that process dynamics changes within the glacier domain. The scale break, when considering snow over the entire glacier in all directions, is of the same order of magnitude as found in other studies, with values between 10 and 35 m. Fractal dimension values before the scale break (D_s) are lower than those after the scale break (D_l), indicating that snow depth has more autocorrelated structure up to a distance of about 20 m over the entire glacier. Lower values of the fractal dimension before the scale break were found also in previous studies that investigated snow depth fractal behavior.
2. Fractal parameters (the fractal dimension and the scale break distance) are similar in the two years, indicating that there is temporal consistency between the accumulation patterns at the end of the winter season. This is in agreement with previous studies on ice-free mountain areas and suggests that the interplay between the factors driving the snow distribution that builds the winter accumulation at the end of the season is consistent from one year to the other also on glaciers. This is a promising result for modeling studies, as it indicates that, once the main factors are identified, one can expect that they exert the same influence over different seasons. Fractal analysis alone cannot provide evidence of the controlling factors, but it seems that these remain, at least over an alpine glacier with size and shape such as Haut Glacier d'Arolla, stable over two seasons.
3. In contrast to the temporal consistency, spatial patterns are markedly different in the ablation area of the glacier tongue and in the upper catchment. Both D_s and L increase from the tongue to the upper areas, suggesting stronger spatial correlation on the tongue. In addition, in the ablation area, we found longer scale break distances and less persistent snow depth distribution in the north-south compare to the east-west direction, while in the upper catchment this distinct behavior is not evident.
4. Previous studies have identified as the key controls on snow scaling properties and spatial correlation either topographic relief, vegetation, or wind. Vegetation is obviously absent on Haut Glacier d'Arolla. We have shown however that wind is a key control of the correlation structure and its anisotropy and directionality. Snow patterns over Haut Glacier d'Arolla seem to be controlled by two scales, one of small-scale interactions and processes and a larger scale of processes determined by the large-scale topographic features of the glacier interacting with the main air flow on the glacier tongue.

The results of this study provide evidence that snow depth distribution on at least some glacier surfaces has similar behavior to snow depth distribution on nonglaciated surfaces, and thus calls for further investigations on the extent of this finding and its main causes. They provide useful information for the spatial and temporal monitoring of snow accumulation patterns on glaciers with similar physical, topographic and flow dynamic characteristics as Haut Glacier d'Arolla and might also be used to support and evaluate snow accumulation modeling in glacierized catchments as they provide indications about the range and temporal behavior of the involved spatial scales.

Acknowledgments
We thank all those who helped for the installation and maintenance of the AWSs and meteorological data collection. Julien Vallet carried out the lidar surveys and preprocessed the data and is gratefully acknowledged. This work is funded by the Swiss National Science Foundation (SNSF) project: "Future glacier evolution and consequences for the hydrology (FUGE)" (Project 4061-40125907), which was part of the SNSF National Research programme NRP 61 "Sustainable water management." We thank Samuel Morin very much for providing the Crocus simulations. The lidar-derived snow depth data sets used in this article can be requested through the ETH Zurich's Research Collection repository (https://doi.org/10.3929/ethz-b-00026 2482). We thank very much Jeffrey S. Deems, Ernesto Trujillo, and an anonymous reviewer for extensive and thorough comments that helped to substantially improve the manuscript, and the Editor Jessica Lundquist for additional very useful comments.

References

Anderton, S. P., White, S., & Alvera, B. (2004). Evaluation of spatial variability in snow water equivalent for a high mountain catchment. *Hydrological Processes*, *18*(3), 435–453.
Arnold, N., & Rees, W. G. (2003). Self-similarity in glacier surface characteristics. *Journal of Glaciology*, *49*(167), 547–554.
Blöschl, G., & Kirnbauer, R. (1992). An analysis of snow cover patterns in a small alpine catchment. *Hydrological Processes*, *6*, 99–109.
Brun, E., David, P., Sudul, M., & Brunot, G. (1992). A numerical model to simulate snow-cover stratigraphy for operational avalanche forecasting. *Journal of Glaciology*, *38*(128), 13–22. https://doi.org/10.3189/S0022143000009552
Brun, E., Martin, E., Simon, V., Gendre, C., & Coleou, C. (1989). An energy and mass model of snow cover suitable for operational avalanche forecasting. *Journal of Glaciology*, *121*, 333–342. https://doi.org/10.3189/S0022143000009254
Burlando, M., Carassale, L., Georgieva, E., Ratto, C., & Solari, G. (2007). A simple and efficient procedure for the numerical simulation of wind fields in complex terrain. *Boundary-Layer Meteorology*, *125*(3), 417–439. https://doi.org/10.1007/s10546-007-9196-3
Clark, M., Hendrikx, J., Slater, A., Kavetski, D., Anderson, B., Cullen, N., et al. (2011). Representing spatial variability of snow water equivalent in hydrologic and land-surface models: A review. *Water Resources Research*, *47*, W07539. https://doi.org/10.1029/2011WR010745
Clemenzi, I. (2016). Understanding and modelling snow accumulation on glaciers (PhD thesis), ETH Zurich. https://doi.org/10.3929/ethz-a-010863699
Dadic, R., Corripio, J. G., & Burlando, P. (2008). Mass-balance estimates for Haut Glacier d'Arolla, Switzerland, from 2000 to 2006 using DEMs and distributed mass-balance modeling. *Annals of Glaciology*, *49*(1), 22–26. https://doi.org/10.3189/172756408787814816
Dadic, R., Mott, R., Lehning, M., & Burlando, P. (2010a). Parameterization for wind-induced preferential deposition of snow. *Hydrological Processes*, *24*(14), 1994–2006. https://doi.org/10.1002/hyp.7776

Dadic, R., Mott, R., Lehning, M., & Burlando, P. (2010b). Wind influence on snow depth distribution and accumulation over glaciers. *Journal of Geophysical Research: Earth Surface*, *115*, F01012. https://doi.org/10.1029/2009JF001261
Deems, J., Fassnacht, S. R., & Elder, K. J. (2006). Fractal distribution of snow depth from lidar data. *Journal of Hydrometeorology*, *7*(2), 285–297.
Deems, J. S., Fassnacht, S. R., & Elder, K. J. (2008). Interannual consistency in fractal snow depth patterns at two Colorado mountain sites. *Journal of Hydrometeorology*, *9*(5), 977–988.
Deems, J. S., Painter, T. H., & Finnegan, D. C. (2013). Lidar measurement of snow depth: A review. *Journal of Glaciology*, *59*(215), 467–479. https://doi.org/10.3189/2013JoG12J154
Egli, L., Jonas, T., Grünewald, T., Schirmer, M., & Burlando, P. (2012). Dynamics of snow ablation in a small alpine catchment observed by repeated terrestrial laser scans. *Hydrological Processes*, *21*(10), 1574–1585. https://doi.org/10.1002/hyp.8244
Elder, K., Dozier, J., & Michaelsen, J. (1991). Snow accumulation and distribution in an alpine watershed. *Water Resources Research*, *27*(7), 1541–1552.
Elder, K., Rosenthal, W., & Davis, R. E. (1998). Estimating the spatial distribution of snow water equivalence in a montane watershed. *Hydrological Processes*, *12*(10-11), 1793–1808.
Erickson, T. A., Williams, M. W., & Winstral, A. (2005). Persistence of topographic controls on the spatial distribution of snow in rugged mountain terrain, Colorado, United States. *Water Resources Research*, *41*, W04014. https://doi.org/10.1029/2003WR002973
Gao, J., & Xia, Z. (1996). Fractals in physical geography. *Progress in Physical Geography*, *20*(2), 178–191. https://doi.org/10.1177/030913339602000204
Gruber, S. (2007). A mass-conserving fast algorithm to parameterize gravitational transport and deposition using digital elevation models. *Water Resources Research*, *43*, W06412. https://doi.org/10.1029/2006WR004868
Helfricht, K., Schöber, J., Schneider, K., Sailer, R., & Kuhn, M. (2014). Interannual persistence of the seasonal snow cover in a glacierized catchment. *Journal of Glaciology*, *60*(223), 889–904. https://doi.org/10.3189/2014JoG13J197
Huss, M., Bauder, A., Funk, M., & Hock, R. (2008). Determination of the seasonal mass balance of four Alpine glaciers since 1865. *Journal of Geophysical Research*, *113*, F01015. https://doi.org/10.1029/2007JF000803
Kerr, T., Clark, M., Hendrikx, J., & Anderson, B. (2013). Snow distribution in a steep mid-latitude alpine catchment. *Hydrological Processes*, *55*, 173–24.
Klinkenberg, B., & Goodchild, M. F. (1992). The fractal properties of topography: A comparison of methods. *Earth Surface Processes and Landforms*, *17*(3), 217–234. https://doi.org/10.1002/esp.3290170303
Lehning, M., Löwe, H., Ryser, M., & Raderschall, N. (2008). Inhomogeneous precipitation distribution and snow transport in steep terrain. *Water Resources Research*, *44*, W07404. https://doi.org/10.1029/2007WR006545
Liston, G. E., Haehnel, R., Sturm, M., Hiemstra, C., Berezovskaya, S., & Tabler, R. (2007). Simulating complex snow distributions in windy environments using SnowTran-3D. *Journal of Glaciology*, *53*(181), 241–256.
Luce, C. H., Tarboton, D. G., & Cooley, K. R. (1998). The influence of the spatial distribution of snow on basin-averaged snowmelt. *Hydrological Processes*, *12*, 1671–1683.
Machguth, H., Paul, F., Hoelzle, M., & Haeberli, W. (2006). Distributed glacier mass-balance modelling as an important component of modern multi-level glacier monitoring. *Annals of Glaciology*, *43*, 335–343.
Mandelbrot, B. (1977). *Fractals: Form, chance, and dimension* (365 pp.). San Francisco: W.H. Freeman.
Mandelbrot, B. (1982). *The fractal geometry of nature* (468 pp.). San Francisco: W.H. Freeman.
Mark, D., & Aronson, P. (1984). Scale-dependent fractal dimensions of topographic surfaces: An empirical investigation, with applications in geomorphology and computer mapping. *Mathematical Geology*, *16*(7), 671–683.
McGrath, D., Sass, L., O'Neel, S., Arendt, A., Wolken, G., Gusmeroli, A., et al. (2015). *Journal of Geophysical Research: Earth Surface*, *120*, 1530–1550. https://doi.org/10.1002/2015JF003539
Mott, R., Schirmer, M., Bavay, M., Grünewald, T., & Lehning, M. (2010). Understanding snow-transport processes shaping the mountain snow-cover. *The Cryosphere*, *4*(4), 545–559.
Nešpor, V., & Sevruk, B. (1999). Estimation of wind-induced error of rainfall gauge measurements using a numerical simulation. *Journal of Atmospheric and Oceanic Technology*, *16*(4), 450–464.
Schirmer, M., & Lehning, M. (2011). Persistence in intra-annual snow depth distribution: 2. Fractal analysis of snow depth development. *Water Resources Research*, *47*, W09517. https://doi.org/10.1029/2010WR009429
Schirmer, M., Wirz, V., Clifton, A., & Lehning, M. (2011). Persistence in intra-annual snow depth distribution: 1. Measurements and topographic control. *Water Resources Research*, *47*, W09516. https://doi.org/10.1029/2010WR009426
Shook, K., & Gray, D. M. (1996). Small scale spatial structure of shallow snowcovers. *Hydrological Processes*, *10*(10), 1283–1292.
Skaloud, J., Vallet, J., Keller, K., Veyssiére, G., & Kölbl, O. (May 2006). An eye for landscapes—Rapid aerial mapping with handheld sensors. *GPS World*, *17 (5)*, 26–32.
Sturm, M., & Wagner, A. M. (2010). Using repeated patterns in snow distribution modeling: An arctic example. *Water Resources Research*, *46*, W12549. https://doi.org/10.1029/2010WR009434
Sun, W., Xu, G., Gong, P., & Liang, S. (2006). Fractal analysis of remotely sensed images: A review of methods and applications. *International Journal of Remote Sensing*, *27*(22), 4963–4990. https://doi.org/10.1080/01431160600676695
Trujillo, E., Ramírez, J., & Elder, K. J. (2007). Topographic, meteorologic, and canopy controls on the scaling characteristics of the spatial distribution of snow depth fields. *Water Resources Research*, *43*, W07409. https://doi.org/10.1029/2006WR005317
Trujillo, E., Ramírez, J., & Elder, K. J. (2009). Scaling properties and spatial organization of snow depth fields in sub-alpine forest and alpine tundra. *Hydrological Processes*, *23*(11), 1575–1590.
Vionnet, V., Brun, E., Morin, S., Boone, A., Faroux, S., Le Moigne, P., et al. (2012). The detailed snowpack scheme crocus and its implementation in SURFEX v7.2. *Geoscientific Model Development*, *5*(3), 773–791. https://doi.org/10.5194/gmd-5-773-2012
Webster, R., & Oliver, M. (2007). *Geostatistics for environmental scientists* (2nd ed.). Chichester, England: John Wiley & Sons Ltd.
Winstral, A., & Marks, D. (2002). Simulating wind fields and snow redistribution using terrain-based parameters to model snow accumulation and melt over a semi-arid mountain catchment. *Hydrological Processes*, *16*, 3585–3603.
Winstral, A., & Marks, D. (2014). Long-term snow distribution observations in a mountain catchment: Assessing variability, time stability, and the representativeness of an index site. *Water Resources Research*, *50*, 293–305. https://doi.org/10.1002/2012WR013038
Winstral, A., Marks, D., & Gurney, R. (2013). Simulating wind-affected snow accumulations at catchment to basin scales. *Advances in Water Resources*, *55*(0), 64–79.
Zweifel, A., & Sevruk, B. (2002). Comparative accuracy of solid precipitation measurements using heated recording gauges in the alps. In *Proc. WCRP Workshop on Determination of Solid Precipitation in Cold Climate Regions*. Fairbanks, Alaska.